

Ag₃PO₄ nanoparticle-decorated Ni/C nanocapsules with tunable electromagnetic absorption properties

Cite as: AIP Advances **7**, 056421 (2017); <https://doi.org/10.1063/1.4975053>

Submitted: 22 September 2016 . Accepted: 02 November 2016 . Published Online: 25 January 2017

Caiyun Cui, Pingping Zhou, Xianguo Liu, Siu Wing Or, and S. L. Ho



View Online



Export Citation



CrossMark

ARTICLES YOU MAY BE INTERESTED IN

Exchange coupling and microwave absorption in core/shell-structured hard/soft ferrite-based CoFe₂O₄/NiFe₂O₄ nanocapsules

AIP Advances **7**, 056403 (2017); <https://doi.org/10.1063/1.4972805>

Interchange core/shell assembly of diluted magnetic semiconductor CeO₂ and ferromagnetic ferrite Fe₃O₄ for microwave absorption

AIP Advances **7**, 055811 (2017); <https://doi.org/10.1063/1.4973204>

Phase-sensitive dc magnetometer based on magnetic–electromagnetic–magnetostrictive–piezoelectric heterostructure

AIP Advances **7**, 056642 (2017); <https://doi.org/10.1063/1.4975133>

AVS Quantum Science

Co-Published by



RECEIVE THE LATEST UPDATES

AIP
Publishing

Ag₃PO₄ nanoparticle-decorated Ni/C nanocapsules with tunable electromagnetic absorption properties

Caiyun Cui,^{1,2} Pingping Zhou,^{1,2} Xianguo Liu,^{1,2,3} Siu Wing Or,^{2,3,a} and S. L. Ho^{2,3}

¹*School of Materials Science and Engineering, Anhui University of Technology, Maanshan 243002, People's Republic of China*

²*Department of Electrical Engineering, The Hong Kong Polytechnic University, Hung Hom, Kowloon, Hong Kong*

³*Hong Kong Branch of National Rail Transit Electrification and Automation Engineering Technology Research Center, Hong Kong*

(Presented 4 November 2016; received 22 September 2016; accepted 2 November 2016; published online 25 January 2017)

Core/shell-structured nickel/carbon (Ni/C) nanocapsules with Ag₃PO₄ nanoparticle decoration (Ag₃PO₄@Ni/C) are prepared by an arc-discharge process and an ion-exchange process. The Ag₃PO₄@Ni/C nanocapsules show a clear decoration of Ag₃PO₄ nanoparticles of 4–20 nm diameter on the C shell of the Ni/C nanocapsules of ~60 nm diameter. The amount of Ag₃PO₄ nanoparticles that can be decorated on the Ni/C nanocapsules depends on the volume of Na₂HPO₄ reactant used in the ion-exchange process. The Ag₃PO₄@Ni/C nanocapsules demonstrate interestingly high and tunable electromagnetic absorption properties with different amounts of Ag₃PO₄ nanoparticle decoration in the paraffin-bonded composites over the 2–18 GHz microwave range. The nanocapsules prepared with 100 ml Na₂HPO₄ exhibit much enhanced dielectric and magnetic losses for an improved electromagnetic impedance match. These result in a large reflection loss (*RL*) of -31.4 dB at 12.3 GHz for a small absorber thickness of 2.6 mm in conjunction with a very wide effective absorption bandwidth (for *RL* < -10 dB) of 14 GHz (4–18 GHz) at a wide absorber thickness range of 1.4–5.0 mm. © 2017 Author(s). All article content, except where otherwise noted, is licensed under a Creative Commons Attribution (CC BY) license (<http://creativecommons.org/licenses/by/4.0/>). [<http://dx.doi.org/10.1063/1.4975053>]

I. INTRODUCTION

The rapid development and utilization of electronic and communication devices have caused serious electromagnetic (EM) radiation and interference problems in our society.¹ High-performance EM absorbers, featuring simultaneously strong absorption, wide absorption bandwidth, small thickness, and low density in the gigahertz microwave range, have become increasingly important and demanding.^{2–4} Core/shell-structured nanocapsules, comprising a magnetic nanoparticle core and a dielectric shell of nanometer size, have attracted considerable attention because of their synergetic effects between dielectric and magnetic losses for absorbing EM waves.^{1–7} Among various types of core/shell-structured nanocapsules, nickel/carbon (Ni/C) nanocapsules are regarded as a high-potential candidate due to their simple material type, simple preparation process, interesting dielectric and magnetic properties, good EM impedance match, and high EM absorption properties, etc.^{1,2,6} For instance, a Ni/C nanocapsule absorber with 2.0 mm thickness exhibits a large reflection loss (*RL*) of ~-32 dB at ~13 GHz and a wide effective absorption bandwidth (for *RL* < -10 dB) of ~4.3 GHz (i.e., 11.2–15.5 GHz).⁶ However, the major obstacle to widespread use of the core/shell-structured nanocapsules in EM absorbers is their almost untunable EM absorption properties constrained by the

^aAuthor to whom correspondence should be addressed. Electronic mail: eeswor@polyu.edu.hk



limited material phase variety in the single core/shell structure.¹ In fact, once the material phases are fixed for the core and the shell in such a nanocapsule (e.g., Ni/C nanocapsule), its EM absorption properties are unable to be further tuned.

Semiconductor materials are known to have complex and rich electronic transport properties.³ By introducing appropriate semiconductor nanoparticles onto/into the core/shell-structured nanocapsules, it can modify their EM absorption properties and lead to new physics. Ag_3PO_4 , which has complex and rich electronic transport properties with a wide bandgap of 2.45 eV, is regarded as a simple and important type of photocatalytic semiconductor materials.² It was recently reported to possess a high relative permittivity of ~ 20 in the 100 Hz–10 MHz range at room temperature due to the existence of a strong space charge polarization.³ By introducing controlled amounts of Ag_3PO_4 nanoparticles onto/into the Ni/C nanocapsules, it is likely to tune/fine-tune their EM absorption properties and to realize tunable EM absorbers.

In this paper, we aim to study the effect of decoration of Ag_3PO_4 nanoparticles on the EM absorption properties of the core/shell-structured Ni/C nanocapsules. Accordingly, Ni/C nanocapsules decorated with different amounts of Ag_3PO_4 nanoparticles (denoted as $\text{Ag}_3\text{PO}_4@/\text{Ni/C}$) are prepared by an arc-discharge process followed by an ion-exchange process. The amount of Ag_3PO_4 nanoparticle decoration is adjusted using different volumes of Na_2HPO_4 reactant in the ion-exchange process. The phase, morphology, microstructure, composition, and charge state of Ni element of the $\text{Ag}_3\text{PO}_4@/\text{Ni/C}$ nanocapsules are investigated, while their EM absorption properties are evaluated in the corresponding paraffin-bonded composites with 50 wt.% $\text{Ag}_3\text{PO}_4@/\text{Ni/C}$ over the 2–18 GHz microwave range. Interestingly high and tunable EM absorption properties are observed and discussed at different amounts of Ag_3PO_4 nanoparticle decoration to provide a new prospective for realizing tunable EM absorbers in general and for fine-tuning their properties to meet application requirements in specific.

II. EXPERIMENTS

Ni/C nanocapsules were prepared by an arc-discharge process.^{1,8} A Ni ingot of 99.9% purity was placed in a water-cooled copper crucible as the anode, while a tungsten needle of 5 mm diameter was employed as the cathode. After evacuating the arc-discharge chamber to 5 mPa, ethanol of 40 ml was introduced into the chamber as the C source. Meanwhile, Ar gas of 20 kPa and H_2 gas of 10 kPa were added into the chamber as the plasma source. An arc-discharge current of 110 A was applied to the chamber for ~ 30 min to ensure a sufficient evaporation of the Ni ingot. The residual gas was then pumped out, and the black powders formed on the inner surface of the chamber were collected as the Ni/C product after they were passivated in N_2 gas for 10 h.

Ag_3PO_4 nanoparticles were prepared on the surface of the as-prepared Ni/C product using an ion-exchange process.⁸ Ni/C product of 0.25 g was dispersed into Na_2HPO_4 hydrate solution of controlled volume under mechanical stirring. AgNO_3 solution of 12 mol/ml was added into the mixture of Ni/C product and Na_2HPO_4 hydrate solution of 3 mol/ml using an $\text{AgNO}_3:\text{Na}_2\text{HPO}_4$ volume ratio of 1:2 at a titration rate of 100 ml/h under vigorous stirring for 1 h. The precipitates were collected by centrifugation, washed several times with distilled water and absolute ethanol, and dried in a vacuum at 60°C for 12 h as the $\text{Ag}_3\text{PO}_4@/\text{Ni/C}$ product. The amount of Ag_3PO_4 nanoparticles being decorated on the Ni/C product was adjusted using different volumes of Na_2HPO_4 reactant. For ease of discussion, the $\text{Ag}_3\text{PO}_4@/\text{Ni/C}$ products (or nanocapsules) prepared in 100, 200, and 300 ml Na_2HPO_4 are denoted as NC_{100} , NC_{200} , and NC_{300} , respectively.

The phase analysis of NC_{100} , NC_{200} , and NC_{300} was performed by an X-ray diffractometer (XRD, Bruker D8 Advance) with monochromatic Cu – $\text{K}\alpha$ radiation ($\lambda = 1.54 \text{ \AA}$). Their morphology and microstructure were evaluated by a transmission electron microscope (TEM, JEOL 2010) at an emission voltage of 200 kV. Their compositions were analyzed using an energy dispersive spectrometer (EDS) integrated with the TEM. The charge state of Ni element in the cores was examined using an X-ray photoelectron spectroscopy (XPS, ESCALAB-250) after the products were etched for 20 s. To enable measurements of the EM absorption properties of NC_{100} , NC_{200} , and NC_{300} , 50 wt.% of NC_{100} , NC_{200} , and NC_{300} was respectively mixed with 50 wt.% of EM wave-transparent liquid paraffin and hexane by ultrasonic waves,¹ and the mixtures were pressed into toroidal composites

with an outer diameter of 7.00 mm, an inner diameter of 3.04 mm, and a thickness of 2.00 mm after the evaporation of hexane. For convenient discussion, the composites fabricated with NC₁₀₀, NC₂₀₀, and NC₃₀₀ are denoted as PC_{NC100}, PC_{NC200}, and PC_{NC300}, respectively. The complex relative permittivity ($\epsilon_r = \epsilon'_r - j\epsilon''_r$) and permeability ($\mu_r = \mu'_r - j\mu''_r$) of PC_{NC100}, PC_{NC200}, and PC_{NC300} were measured by a transmission/reflection coaxial line method in the 2–18 GHz microwave range covering the full S, C, X, and Ku bands of microwaves using a vector network analyzer (Anritsu 37269D) with short, open, load, and thru calibrations. The frequency (f) dependence of reflection loss (RL) was determined from the measured ϵ_r and μ_r spectra using¹

$$RL = 20\log|(Z_{in} - Z_0)/(Z_{in} + Z_0)| \quad (1)$$

where $Z_{in} = Z_0(\mu_r/\epsilon_r)^{1/2} \tanh[j(2\pi fd/c)(\mu_r\epsilon_r)^{1/2}]$ is the input impedance of composite, $Z_0 \sim 377 \Omega$ is the characteristic impedance of air, $c=3\times 10^8$ m/s is the velocity of light, and d is the thickness of composite.

III. RESULTS AND DISCUSSION

Figure 1 shows the XRD patterns of typical NC₁₀₀, NC₂₀₀, and NC₃₀₀. The Ni phase is identified by the characteristic diffraction peaks of Ni (JCPDS card No. 04-0850), while the other diffraction peaks match well with the body-centered cubic phase of Ag₃PO₄ (JCPDS card No. 06-0505). The observation suggests a constitution of Ni and Ag₃PO₄ in the Ag₃PO₄@Ni/C products. The intensity ratio of Ni (111) peak to Ag₃PO₄ (210) peak in NC₁₀₀, NC₂₀₀, and NC₃₀₀ is found to be 1.34, 1.00, and 0.55, respectively, indicating an increase in the amount of Ag₃PO₄ nanoparticle decoration with increasing the volume of Na₂HPO₄ reactant used for preparing NC₁₀₀ (100 ml), NC₂₀₀ (200 ml), and NC₃₀₀ (300 ml) in the ion-exchange process. The weaker Ag₃PO₄ diffraction peaks in NC₁₀₀ and then NC₂₀₀ compared to NC₃₀₀ implies the existence of a lower degree of crystallization in Ag₃PO₄ for NC₁₀₀ and NC₂₀₀ than for NC₃₀₀. No diffraction peaks in relation to Ni oxides are detected in all products so that the C shells are effective in protecting the Ni cores from oxidation.^{1,7} Also, no diffraction peaks are observed for C due to the breaking of the translational symmetry along the radial direction.^{1,7}

Figures 2(a), 2(b), and 2(c) illustrate the TEM images of typical NC₁₀₀, NC₂₀₀, and NC₃₀₀, respectively. It is clear that NC₁₀₀, NC₂₀₀, and NC₃₀₀ consist of different amounts of small spherical nanoparticles of 4–20 nm diameter decorated on the surface of the relatively larger spherical nanoparticle of ~60 nm diameter. Our in-situ TEM observation found that the amount of small nanoparticle decoration increases from 12 in NC₁₀₀ to 25 in NC₂₀₀ and then 35 in NC₃₀₀ (not shown), so that it can be effectively controlled by the volume of Na₂HPO₄ reactant adopted in the ion-exchange process. The diameter of the small nanoparticles was observed to be 4–6 nm in NC₁₀₀, 15–20 nm in NC₂₀₀, and 8–15 nm in NC₃₀₀. The reason why NC₃₀₀ has smaller particle sizes than NC₂₀₀ may be

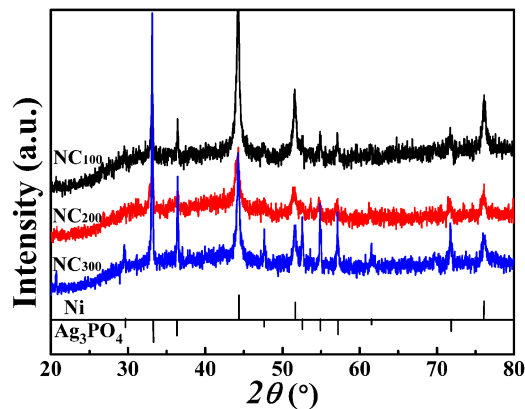


FIG. 1. XRD patterns of typical NC₁₀₀, NC₂₀₀, and NC₃₀₀.

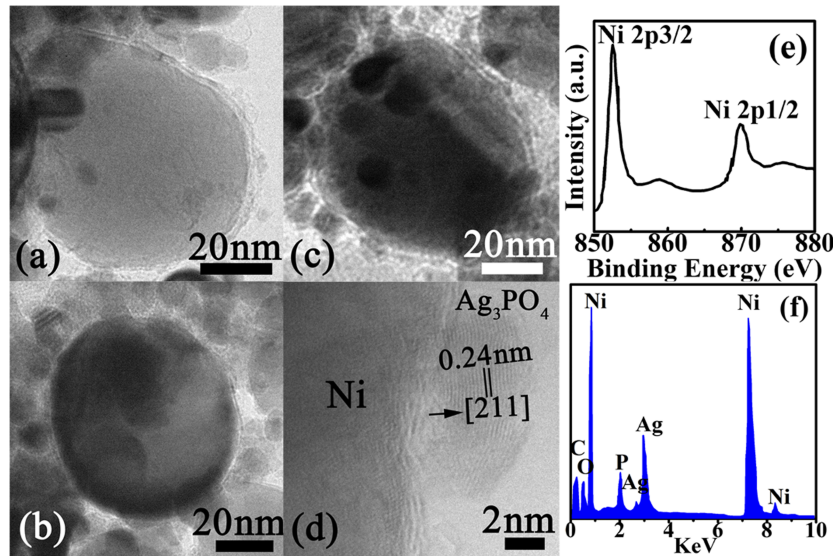


FIG. 2. TEM images of typical (a) NC₁₀₀, (b) NC₂₀₀, and (c) NC₃₀₀. (d) HRTEM image of NC₁₀₀ in (a). (e) Typical XPS spectrum of the Ni cores after etching NC₁₀₀ for 20 s. (f) Typical EDS pattern of NC₁₀₀.

explained by the saturation of solutions under the given concentrations and conditions. Figure 2(d) displays the HRTEM image of NC₁₀₀ in Fig. 2(a). It is seen that a small spherical nanoparticle of ~5 nm diameter is firmly grown on the shell of a relatively larger spherical nanoparticle having a typical core/shell structure in which the nanoparticle core is encapsulated by an onion-like shell of ~2 nm thickness. The variation of onion-like shell thickness was found to have no obvious correlation with the nanoparticle core size based on statistical approach. Nonetheless, the lattice plane spacing of the decorated small nanoparticles is found to be ~0.24 nm. This value agrees with the *d*-spacing of {211} planes of Ag₃PO₄, confirming the successful preparation of Ag₃PO₄ nanoparticles of 4–20 nm diameter on the C shell of the Ni/C nanocapsules of ~60 nm diameter. Figure 2(e) gives a typical XPS spectrum of the Ni cores after etching NC₁₀₀ for 20 s. The two XPS peaks observed at 582.5 and 870.0 eV, corresponding to the Ni 2p_{3/2} and Ni 2p_{1/2} electron states, respectively, indicate the existence of zero charge state of Ni element in the Ni cores. Figure 2(f) provides a typical EDS pattern of NC₁₀₀. The detection of Ag, P, O, Ni, and C elements further evidences the co-existence of Ag₃PO₄ and Ni/C in our Ag₃PO₄@Ni/C products.

Figure 3(a) shows the measured *f* dependence of $\epsilon_r = \epsilon'_r - j\epsilon''_r$ of PC_{NC100}, PC_{NC200}, and PC_{NC300}. Recalling that ϵ'_r and ϵ''_r represent the amount of polarization and the level of energy dissipation, respectively,⁹ ϵ'_r and ϵ''_r of all composites demonstrate similar quantitative decreasing trends with increasing *f* in the 2–6 GHz range, except for the broad dielectric resonance in the 6–18 GHz range. The weakening of the ϵ'_r and ϵ''_r responses is mainly caused by the lagging of dipole polarization response with respect to the change in electric field at elevated frequencies.^{7,10} This is the typical behavior of a dielectric material outside the vicinity of a dielectric resonance. Following the effective-medium theory of three-phase inclusions, the dielectric resonance behavior originates mainly from the special geometries and structures of the inclusions of Ag₃PO₄@Ni/C nanocapsules, the intrinsic permittivity of each component in the composite (e.g., Ni, C, Ag₃PO₄, and paraffin), and the dispersion of the nanocapsules.^{1,11} Nevertheless, the values of ϵ'_r and ϵ''_r in PC_{NC100} are generally larger than those of PC_{NC300} and PC_{NC200}. According to the free electron theory,¹² $\epsilon''_r \approx 1/2\pi\rho f$, where ρ is the resistivity. A small ϵ''_r implies a high ρ . The largest ϵ''_r in PC_{NC100} compared to PC_{NC300} and then PC_{NC200} indicates the presence of the lowest ρ in PC_{NC100} than in PC_{NC300} and then in PC_{NC200}. As the effective ρ depends on the distance between Ni/C nanocapsules, the size of Ag₃PO₄ nanoparticles shall have the determinative effect on the effective ρ . Therefore, the use of smaller sized Ag₃PO₄ nanoparticles can induce a lower ρ and hence a larger ϵ''_r .

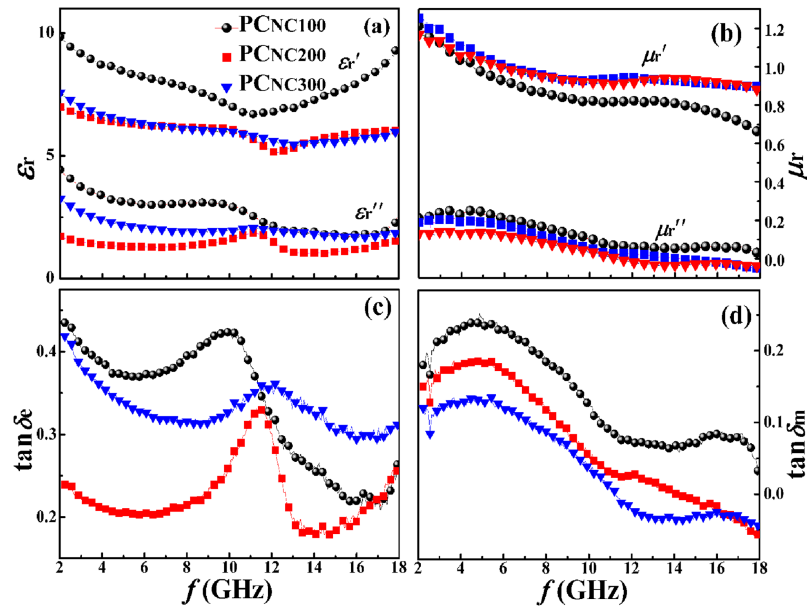


FIG. 3. Measured f dependence of (a) $\epsilon_r = \epsilon_r' - j\epsilon_r''$ and (b) $\mu_r = \mu_r' - j\mu_r''$ as well as calculated f dependence of (c) $\tan \delta_e = \epsilon_r''/\epsilon_r'$ and (d) $\tan \delta_m = \mu_r''/\mu_r'$ for PC_{NC100}, PC_{NC200}, and PC_{NC300}.

Figure 3(b) shows the measured f dependence of $\mu_r = \mu_r' - j\mu_r''$ of PC_{NC100}, PC_{NC200}, and PC_{NC300}. μ_r' of all composites shows similar quantitative decreasing trends in the 2–18 GHz range due to the relaxation of magnetic moment precession.^{6,7} However, μ_r'' of all composites increases slightly in the 2–4.3 GHz range and then decreases in the 4.3–18 GHz range because the magnetic resonance peaks at ~ 4 GHz. It is noted that μ_r' of PC_{NC100} is smaller than that of PC_{NC200} and PC_{NC300}, especially for $f > 10$ GHz. This is because the amount of Ag₃PO₄ nanoparticle decoration in PC_{NC100} is relatively few (i.e., 12 for NC₁₀₀, 25 for NC₂₀₀, and 35 for NC₃₀₀) and the decorated Ag₃PO₄ nanoparticles are not strong enough to protect the magnetic Ni cores in the 10 GHz range. However, μ_r'' of PC_{NC100} is larger than that of PC_{NC200} and PC_{NC300} since the decoration of Ag₃PO₄ nanoparticles can dilute the effective magnetic response in the gigahertz range. In a general sense, the magnetic loss in a magnetic material can be attributed to domain-wall displacement, eddy-current loss, natural resonance, and/or exchange resonance.¹ The domain-wall resonance occurs only in multi-domain materials in the 1–100 MHz range.⁹ The eddy-current loss is usually excluded because of the size effect.¹ The exchange resonance happens in the high-frequency microwave range in excess of 10 GHz in accordance with Aharoni's theory.⁹ Thus, the magnetic resonance observed at ~ 4 GHz is mainly due to natural resonance.

Figures 3(c) and 3(d) show the calculated f dependence of dielectric loss tangent ($\tan \delta_e = \epsilon_r''/\epsilon_r'$) and magnetic loss tangent ($\tan \delta_m = \mu_r''/\mu_r'$) of PC_{NC100}, PC_{NC200}, and PC_{NC300} based on the data in Figs. 3(a) and 3(b), respectively. These loss tangents are the main loss contributors to the absorption ability of an EM absorber.⁷ The higher the value, the larger the loss is. It should be noted that $\tan \delta_e$ of all composites in Fig. 3(c) exhibits similar quantitative trends with their respective ϵ_r'' in Fig. 3(a). This similarity supports our previous discussion that the size of Ag₃PO₄ nanoparticles has a crucial role in determining ρ and hence ϵ_r'' and $\tan \delta_e$. On the other hand, $\tan \delta_m$ in Fig. 3(d) decreases steadily with increasing the amount of Ag₃PO₄ nanoparticle decoration so that it can be effectively tuned by the amount of Ag₃PO₄ nanoparticle decoration. Both $\tan \delta_e$ and $\tan \delta_m$ are generally larger in PC_{NC100} than in PC_{NC200} and PC_{NC300}, suggesting the existence of a higher EM absorption ability in PC_{NC100}.

Figures 4(a), 4(b), and 4(c) give the calculated 3D RL - f - d mapping plots for PC_{NC100}, PC_{NC200}, and PC_{NC300} in the d range of 1–10 mm with 0.1 mm interval based on Eq. (1), while Figs. 4(d), 4(e), and 4(f) display the RL spectra extracted from Figs. 4(a), 4(b), and 4(c), respectively, at some selected d . It is clear that the optimized RL as strong as -31.4 dB is located at 12.3 GHz and 2.6 mm

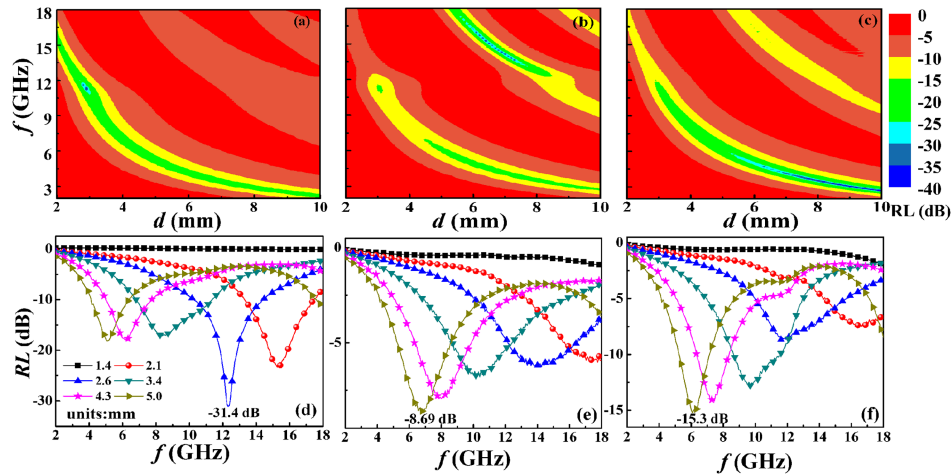


FIG. 4. Calculated 3D RL - f - d mapping plots for (a) PC_{NC100}, (b) PC_{NC200}, and (c) PC_{NC300} in the d range of 1–10 mm. Extracted RL spectra for (d) PC_{NC100}, (e) PC_{NC200}, and (f) PC_{NC300} at some selected d .

in PC_{NC100}, but it is significantly weaker at lower f and larger d in both PC_{NC200} (-8.69 dB at 6.4 GHz and 5.0 mm) and PC_{NC300} (-15.2 dB at 6.1 GHz and 5.0 mm). PC_{NC100} demonstrates the most superior EM absorption performance, and this is followed by PC_{NC300} and PC_{NC200}, for the same d of 2.6 mm. Moreover, the effective absorption bandwidth for $RL < -10$ dB, corresponding to 90% absorption, is as wide as 14 GHz in PC_{NC100}, covering the whole C (4–8 GHz), X (8–12 GHz), and Ku (12–18 GHz) microwave bands and involving a broad range of d of 1.4–5.0 mm. In general, the optimal RL value and the effective absorption bandwidth of our samples exhibit a downward trend with an increase in the amount and/or size of Ag₃PO₄ nanoparticles. For comparison, Ni/C nanocapsule composites without any decoration have comparable optimized RL of -32 dB at 13 GHz and 2.0 mm at the expense of much narrower effective absorption bandwidth of 4.3 GHz in the 11.2–15.5 GHz range.⁶

Recalling that the EM absorption performance of an absorber relies on the degree of EM impedance match, which can be characterized by the delta function expressed as $\Delta = |\sinh^2(Kfd)M|$, where K and M depends on ϵ_r and μ_r .¹⁰ A smaller Δ value implies a higher degree of EM impedance match. Figure 5 presents the calculated 3D Δ - f - d mapping plots of PC_{NC100}, PC_{NC200}, and PC_{NC300}. The Δ values in PC_{NC100} are generally less than 0.6 (blue areas) (Fig. 5(a)), reflecting the presence of a high degree of EM impedance match. The degree of EM impedance match is comparatively lower in PC_{NC300} and then in PC_{NC200} (Figs. 5(b) and 5(c)). It is noted that these 3D Δ - f - d mapping plots show very similar tendency with the 3D RL - f - d mapping plots in Fig. 4. The high similarity confirms that the enhancement in EM absorption performance in PC_{NC100} is a result of the enhanced

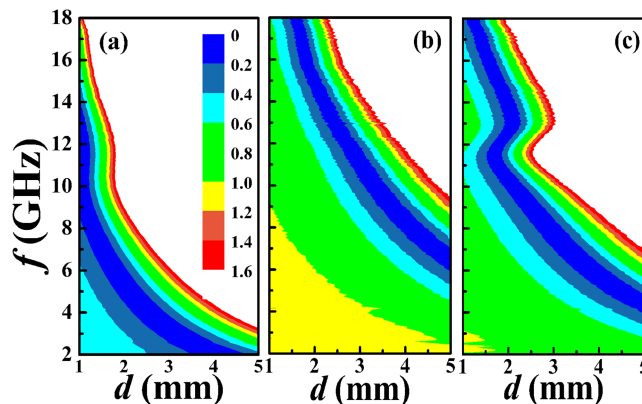


FIG. 5. Calculated 3D Δ - f - d mapping plots of (a) PC_{NC100}, (b) PC_{NC200}, and (c) PC_{NC300}.

dielectric and magnetic losses for an improved EM impedance match via the decoration of an appropriate amount of Ag_3PO_4 nanoparticles onto the Ni/C nanocapsules by using an appropriate volume of Na_2HPO_4 reactant in the ion-exchange process. Ag_3PO_4 nanoparticles may play a dual role in this case. First, they adjust the impedance between permittivity and permeability to make more EM waves traveling into the absorber. Second, they introduce additional interfaces to enhance dielectric and magnetic losses in the absorber.

IV. CONCLUSION

We have applied an arc-discharge method and an ion-exchange method to prepare three different types of Ag_3PO_4 nanoparticle-decorated, core/shell-structured Ni/C nanocapsules (Ag_3PO_4 @Ni/C nanocapsules, denoted as NC_{100} , NC_{200} , and NC_{300}) having three different amounts of Ag_3PO_4 nanoparticles (12, 25, and 35) using three different volumes of Na_2HPO_4 reactant (100, 200, and 300 ml) in the ion-exchange process. We have also investigated the phase, morphology, microstructure, composition, and charge state of Ni element of NC_{100} , NC_{200} , and NC_{300} in addition to evaluating their EM absorption properties in the corresponding paraffin-bonded composites ($\text{PC}_{\text{NC}100}$, $\text{PC}_{\text{NC}200}$, and $\text{PC}_{\text{NC}300}$) in the 2–18 GHz microwave range. The Ag_3PO_4 @Ni/C nanocapsules have been found to have a clear decoration of Ag_3PO_4 nanoparticles of 4–20 nm diameter on the C shell of the Ni/C nanocapsules of ~60 nm diameter as well as an interestingly high and tunable EM absorption properties with different amounts of Ag_3PO_4 nanoparticle decoration. Among them, the one prepared with 100 ml Na_2HPO_4 (NC_{100} or $\text{PC}_{\text{NC}100}$) has exhibited much enhanced dielectric and magnetic losses for an improved EM impedance match, giving rise to a large RL of -31.4 dB at 12.3 GHz and 2.6 mm as well as a very wide effective absorption bandwidth (for $RL < -10$ dB) of 14 GHz (4–18 GHz) at a wide d range of 1.4–5.0 mm. This tunable effect has been discussed to provide a new prospective for realizing tunable EM absorbers.

ACKNOWLEDGMENTS

This work was supported by the Innovation and Technology Commission of the HKSAR Government to the Hong Kong Branch of National Rail Transit Electrification and Automation Engineering Technology Research Center (1-BBYF), The Hong Kong Polytechnic University (G-YBLL), and the National Training Program of Innovation and Entrepreneurship for College Student (201510360008).

- ¹ N. D. Wu, X. G. Liu, C. Y. Zhao, C. Y. Cui, and A. L. Xia, *J. Alloys Compd.* **656**, 628 (2016).
- ² G. X. Zhu, X. W. Wei, and S. Jiang, *J. Mater. Chem.* **17**, 2301 (2007).
- ³ M. Thomas, S. K. Ghosh, and K. C. George, *Indian J. Phys.* **77A**, 425 (2003).
- ⁴ B. C. Wang, J. L. Zhang, T. Wang, L. Qiao, and F. S. Li, *J. Alloys Compd.* **567**, 21 (2013).
- ⁵ P. Xu, X. Han, C. Wang, D. Zhou, Z. Lv, A. Wen, and B. Zhang, *J. Phys. Chem. B* **112**, 10443 (2008).
- ⁶ X. F. Zhang, X. L. Dong, H. Huang, Y. Y. Liu, W. N. Wang, X. G. Zhu, and C. G. Lee, *Appl. Phys. Lett.* **89**, 3115 (2006).
- ⁷ X. G. Liu, S. W. Or, C. M. Leung, and S. L. Ho, *J. Appl. Phys.* **115**, 17A507 (2014).
- ⁸ C. Y. Cui, P. P. Zhou, N. D. Wu, Y. H. Lv, and X. G. Liu, *Mater. Lett.* **161**, 325 (2015).
- ⁹ B. Lu, X. L. Dong, H. Huang, X. F. Zhang, X. G. Zhu, and J. P. Lei, *J. Magn. Mater.* **320**, 1106 (2008).
- ¹⁰ Z. Ma, C. T. Cao, Q. F. Liu, and J. B. Wang, *Chin. Phys. Lett.* **29**, 038401 (2012).
- ¹¹ Z. H. Wang, Z. Han, D. Y. Geng, and Z. D. Zhang, *Chem. Phys. Lett.* **489**, 187 (2010).
- ¹² J. Xiang, J. L. Li, X. H. Zhang, Q. Ye, J. H. Xu, and X. Q. Shen, *J. Mater. Chem. A* **2**, 16905 (2014).